

Automatic Calibration Method for Mounting Position of Protein Crystal Mounting Robot Based on Visual Positioning

Jiangping Qin

Shanghai Institute of Applied Physics Chinese Academy of Sciences <https://orcid.org/0000-0002-1192-0326>

Zhaolong Li

Shanghai Institute of Applied Physics Chinese Academy of Sciences

Bo Sun

Shanghai Advanced Research Institute

Feng Yu

Shanghai Advanced Research Institute

Yi Liu

Shanghai Institute of Applied Physics Chinese Academy of Sciences

Kunhao Zhang

Shanghai Advanced Research Institute

Qisheng Wang (✉ wangqs@sari.ac.cn)

Shanghai Institute of Applied Physics Chinese Academy of Sciences

Original Article

Keywords: Protein crystal automounting robot, monocular vision, visual positioning, automatic calibration

Posted Date: December 10th, 2020

DOI: <https://doi.org/10.21203/rs.3.rs-122417/v1>

License: © ⓘ This work is licensed under a Creative Commons Attribution 4.0 International License.

[Read Full License](#)

Abstract

With the popularization of automounting robots in protein crystal diffraction experiment beamline stations, the coordinate calibration of the robot sample mounting position has become an inevitable task in the daily maintenance of the beamline station. In this method, the image features of the laser sensor spot and goniometer are extracted by color extraction and edge detection, respectively, and the noise is eliminated by median filtering. Then, after locating the pixel coordinates of the center of the circle through the Hough circle detection and the minimum closed circle fitting algorithm, the coordinates in the base coordinate system are obtained using the camera internal and external parameter matrices and the hand-eye relationship matrix. Finally, according to the deviation of the laser spot and the visual positioning coordinate of the goniometer, the position of the robot is compensated to improve the positioning accuracy, and the automatic calibration of the sample point is realized.

1 Introduction

Life sciences, especially the determination of the structure and function of biological macromolecules targeting proteins, have laid an important theoretical foundation for studying the nature and activity rules of life phenomena. In the research of life sciences, structural biology with protein crystallography as the main method has developed rapidly. The number and scale of research groups are also increasing rapidly. The demand for corresponding crystallographic diffraction experiments has increased dramatically. These experiments are currently mainly completed on the crystallography beamline at a third-generation synchrotron radiation facility[1]. In order to solve the gap in the demand for experimental machines, the major international crystallographic beamline end-stations began to use automatic mounting robot system instead of manual mounting[2–5], which not only increased the safety of the experiment, but also greatly improved the experimental efficiency.

The protein crystal automatic mounting robot system needs to realize three functions, sample storage, sample acquisition and sample transfer. Before the diffraction experiment, the robot obtains the stored protein crystal sample from the designated position (sample point) in the liquid nitrogen dewar, and then transfers the sample to the goniometer (sample loading point) of the diffractometer. After the diffraction experiment, the robot will remove the sample, put it back in the liquid nitrogen Dewar, and then transfer the next sample to the goniometer[6, 7]. In the process of sample acquisition and sample transfer, the sample point and sample loading point need to be calibrated in advance. After the calibrated coordinates are recorded into the robot controller, sample grabbing and sample loading operations can be performed according to the calibrated coordinates. Coordinate calibration requires manual teaching to move the robot to the target point[8, 9], and then complete the change of the global coordinate variables of the target point through the corresponding control program in the robot controller. With the operation of the system, there will be slight deviations between the calibration position and the actual position of the hardware. Therefore, during regular operation and maintenance, the coordinate points need to be recalibrated to ensure the positioning accuracy of the system and ensure the safety of the experiment.

In the protein crystal automatic sample loading system, the diffractometer goniometer and the automatic mounting robot are on different tables, and the diffractometer is also a device that can be translated with three degrees of freedom. As the experiment progresses, there will be accumulation of positional deviations, so the calibration and maintenance of its coordinates are particularly frequent. In view of this situation, this paper introduces a way of using visual positioning to realize the automatic calibration of the loading position of the protein crystal robot.

2 System Hardware Structure

This method uses an industrial camera to complete the visual positioning, which does not require industrial cameras with high imaging quality. Therefore, Huateng CMOS industrial camera with 5 million pixels is selected as the vision sensor, and Huateng HTF0818-5MP lens with a focal length of 8 mm is configured. The specific parameters of Huateng HT-SUA500C-T industrial camera and HTF0818-5MP lens are shown in table 1 and Table 2:

Table 1
HT-SUA500C-T industrial camera parameters

adapter	Resolution	pixel	pixel size/ μm	lens mount
USB 3.0	2592 × 1944	5 million	2.2 × 2.2	C

Table 2
HTF0818-5MP lens parameters

Focal Length/mm	aperture	lens mount	field angle (H × V × D)
8	F = 2.0-C	C	42.1° × 38.2° × 52.1°

Since the goniometer can move in the X, Y, and Z directions, as shown in Fig. 1, the depth information of the photo cannot be judged for monocular vision as shown in Fig. 1, so the Z-axis coordinates of the goniometer cannot be determined.

On the one hand, the addition of a laser ranging sensor can measure depth information, and on the other hand, can use the deviation of the laser point and the center of the goniometer to correct the error of visual positioning. The parameters of the laser ranging sensor are shown in Table 3:

Table 3
Panasonic HG-C1100 laser ranging sensor parameters

Measuring center distance	measuring range	repeatability	linearity	temperature characteristic
100 mm	± 35 mm	70 μm	± 0.1% FS	0.03% FS/°C

For the recognition and positioning of the goniometer head due to its small size and compact environment, if the camera is far away, it will affect the accuracy of visual positioning, and the robot may block the view when the gripper is close to the target, causing the goniometer head to be blocked and interfere with recognition Positioning. Therefore, this method adopts the "Eye-in-Hand" type hand-eye system to fix the industrial camera on the robot flange to collect image information.

3 Feature Extraction And Positioning Of Laser And Goniometer

3.1 Camera parameter calibration

As shown in Fig. 2, the camera imaging process can be expressed as the conversion of image points in the world coordinate system, camera coordinate system, retinal coordinate system, and pixel coordinate system[10, 11].

It can be seen from Fig. 2 that a point P_w in the world coordinate system needs to be transformed by 4 coordinate systems before it can be represented by pixel coordinates in the imaging plane. According to the principle of homogeneous coordinate transformation, the mapping relationship between the pixel coordinate system and the world coordinate system can be obtained, as shown in formula (1):

$$Z_c \begin{bmatrix} u \\ v \\ 1 \end{bmatrix} = \begin{bmatrix} \frac{f}{dx} & 0 & u_0 & 0 \\ 0 & \frac{f}{dy} & v_0 & 0 \\ 0 & 0 & 1 & 0 \end{bmatrix} \begin{bmatrix} C_R & C_P \\ 0 & 1 \end{bmatrix} \begin{bmatrix} X_w \\ Y_w \\ Z_w \\ 1 \end{bmatrix} = \mathbf{AM} \begin{bmatrix} X_w \\ Y_w \\ Z_w \\ 1 \end{bmatrix} \quad (1)$$

\mathbf{A} is the internal parameter matrix of camera, which is determined by the camera's internal properties. \mathbf{M} is the external parameter matrix of camera, which describes the pose relationship between the camera coordinate system and the world coordinate system.

Through the calibration algorithm that was put forward by Zhang Zhengyou[12], the corresponding internal and external parameter matrix can be obtained by using a two-dimensional checkerboard calibration board. In this paper, the camera is calibrated by the MATLAB camera calibration tool, and the internal parameters of the camera are shown in Table 4.

Table 4
Camera internal reference

f_x	f_y	u_0	v_0
1806.276	1805.866	313.818	218.459

3.2 Hand-eye calibration

The most important step of the combined application of machine vision on industrial robots is hand-eye calibration. The purpose of hand-eye calibration is to realize the transformation of objects in the world coordinate system and the robot coordinate system, so that the robot can perform the corresponding pose transformation according to the image information.

Through the Tsai-Lenz hand-eye calibration algorithm, the hand-eye relationship matrix ${}^E_C T$ of the visual system of "Eye-in-Hand" type[13] is obtained:

$${}^E_C T = \begin{bmatrix} 0.9968 & -0.0723 & 0.0338 & 62.2114 \\ 0.0735 & 0.9966 & -0.0362 & 1.0864 \\ -0.0311 & 0.0386 & 0.9988 & 423.3725 \\ 0 & 0 & 0 & 1 \end{bmatrix} \quad (2)$$

The hand-eye relationship matrix represents the transformation matrix from the camera coordinate system to the robot end coordinate system.

3.3 Image feature extraction and positioning

The visual positioning of the system has two research objects, namely the goniometer and the laser sensor spot. The outer contours of the two can be approximated as circles with diameters of 9 mm and 0.8 mm respectively. The positioning images of both research objects are shown in Fig. 4.

Since the center of the laser spot has a high brightness and is quite different from the surrounding environment, the spot image is extracted according to the color characteristics. Compared with other image visual features, color features are less dependent on image orientation, viewing angle, size and other conditions, so they have higher robustness. First, the HSV color threshold of the laser spot center is determined. Set the upper and lower limits of the threshold by extracting the HSV parameters of the pixel points in the center of the light spot to (0,0,240), (170,20,255), respectively, and traverse the pixels of the entire image. The pixel values that are less than lower limit or greater than upper limit of the threshold are set to 0, and the pixels values in the threshold area are set to 255, and the ROI mask of the image can be obtained.

The mask and the original image are combined to extract the laser spot image, as shown in Fig. 3(a). There will be some noise in the obtained laser spot feature image. In order to eliminate the noise, median filtering was performed on the image to obtain a smoother spot image, as shown in Fig. 3(b).

After the positioning images of laser sensor spot are obtained, it is necessary to obtain the positioning images of goniometer. Using the minimum closed circle fitting algorithm and Hough circle detection[14, 15] algorithm of opencv, the laser spot and the goniometer image can be delineated by the closed circle, and the pixel coordinate position of the circle center can be determined as shown in Fig. 3(c) and Fig. 3(d):

After obtaining the pixel coordinates of the center of the circle, according to formula 1, the coordinates of the corresponding laser spot and goniometer in the camera coordinate system can be solved, and the coordinates in the tool coordinate system of mechanical arm can be obtained through the hand-eye relationship matrix (as shown in formula 2), so as to achieve coordinate positioning.

Three sets of visual positioning experiments are carried out on the goniometer to determine its positioning error. The real coordinate values come from the coordinate position of manual calibration. The experimental results are shown in Table 5:

Table 5
Experimental error of visual positioning of goniometer center

number	positioning coordinate /(mm)		real coordinate /(mm)		positioning error /(mm)	
	X	Y	X	Y	X	Y
	1	812.92	335.66	811.16	334.23	1.76
2	802.03	327.88	800.44	326.25	1.59	1.73
3	820.14	342.83	818.46	341.06	1.68	1.77

It can be seen from Table 5 that the average error of the center coordinates of the goniometer in the X and Y directions only by monocular vision positioning are 1.68 mm and 1.61 mm respectively, which far exceed the error range allowed by the position calibration of the above sample points.

4 Compensation For Deviation Of Visual Positioning Using Laser

Since the error of monocular vision positioning is about 1.6 mm, although it cannot meet the requirements of coordinate calibration, it is enough to ensure that the spot of laser ranging sensor on the gripper falls on the goniometer. The height information of the goniometer can be measured to determine The Z axis coordinate value of the goniometer. By adjusting the height of the gripper, the gripper is pd at the specified height above the goniometer, and then the next image acquisition and positioning can be carried out. The positioning accuracy of the height value is determined by the hardware performance of the laser ranging sensor. The precision of the laser ranging sensor that is selected in this paper can reach 70 μm .

The pixel coordinates of the light spot and the center of the goniometer are identified, and the coordinate deviation value is obtained. According to formula 1, the corresponding coordinate deviation in the camera coordinate system is solved, and the real coordinate deviation is obtained through the hand-eye relationship matrix. Finally, the coordinate deviation value is transferred to control the robot for position compensation. The visual control block diagram of the automatic calibration of the position of the goniometer at the sample point is shown in Fig. 4:

Move the goniometer to different positions to perform 3 sets of automatic calibration experiments, and then manually teach to find the true position, and measure the calibration error, as shown in Table 6:

Table 6
Automatic calibration error of goniometer

number	Calibration coordinate value		real coordinate		positioning error	
	/(mm)		/(mm)		/(mm)	
	X	Y	X	Y	X	Y
1	823.15	322.24	822.83	322.01	0.32	0.23
2	817.37	319.56	817.02	319.30	0.35	0.26
3	811.68	320.35	811.41	320.16	0.27	0.19

It can be seen that the average error of plane coordinates X and Y of the three sets of visual positioning data after one offset compensation are 0.313 mm and 0.227 mm.

5 Conclusion

In this paper, the combination of laser ranging sensor and monocular vision positioning is used to realize the positioning of the three-dimensional XYZ coordinates of the goniometer, and the deviation of the spot position and the center of the goniometer is compensated to improve the vision calibration accuracy of the goniometer. Compared with the simple use of visual positioning, the positioning accuracy of the plane X and Y directions using the laser spot deviation compensation method is improved to 0.313 mm and 0.227 mm, which can be used to realize the automatic positioning of the sample loading position.

Declarations

Acknowledgements

We thank the staffs of beamline BL17U1 at Shanghai Synchrotron Radiation Facility (SSRF), beamlines BL18U1 and BL17B at National Facility for Protein Sciences (NFPS) for equipment support and technology guidance.

Authors' Contributions

ZL was in charge of the design of visual positioning algorithm. BS and QW conceived some ideas. JQ and ZL completed the test of the algorithm. JQ and ZL wrote the manuscript. YF, YL and KZ gave some advices on the manuscript. All authors read and approved the final manuscript.

Funding

supported by Youth Innovation Promotion Association of China (Grant No.2018299).

Competing Interests

The authors declare no competing financial interests.

References

1. Q Wang, F Yu, S Huang, et al. The macromolecular crystallography beamline of SSRF. *Nuclear Science and Techniques*, 2015, 26(1): 8-13.
2. F Cipriani, F Felisaz, L Launer, et al. Automation of sample mounting for macromolecular crystallography. *Acta Crystallogr D Biol Crystallogr*, 2006, 62(10): 1251-1259. doi:10.1107/S0907444906030587.
3. S Russi, J Song, S E McPhillips, et al. The Stanford Automated Mounter: pushing the limits of sample exchange at the SSRL macromolecular crystallography beamlines. *J Appl Crystallogr*, 2016, 49(2): 622-626. doi:10.1107/S1600576716000649.
4. D Nurizzo, M W Bowler, H Caserotto, et al. RoboDiff: combining a sample changer and goniometer for highly automated macromolecular crystallography experiments. *Acta Crystallogr D Struct Biol*, 2016, 72(8): 966-75. doi:10.1107/S205979831601158X.
5. G Papp, F Felisaz, C Sorez, et al. FlexED8: the first member of a fast and flexible sample-changer family for macromolecular crystallography. *Acta Crystallogr D Struct Biol*, 2017, 73(10): 841-851. doi:10.1107/S2059798317013596.
6. M Hiraki, N Matsugaki, Y Yamada, et al. Development of sample exchange robot PAM-HC for beamline BL-1A at the photon factory. *AIP Conference Proceedings*, 2016. doi: 10.1063/1.4952852
7. H Murakami, K Hasegawa, G Ueno, et al. Development of SPACE-II for rapid sample exchange at SPring-8 macromolecular crystallography beamlines. *Acta Crystallographica Section D*, 2020, 76: 155-165. doi:10.1107/S2059798320000030.
8. H Deng, H Wu, C Yang, et al. Base frame calibration for multi-robot coordinated systems. *2015 IEEE International Conference on Robotics and Biomimetics*, Zhuhai, China, December 6-9, 2015: 1489-1494. doi:10.1109/ROBIO.2015.7418981.

9. G Chen, H Wang and Z Lin. Determination of the Identifiable Parameters in Robot Calibration Based on the POE Formula. *IEEE Transactions on Robotics*, 2014, 30(5): 1066-1077. doi:10.1109/tro.2014.2319560.
10. X Wang, H Chen, Y Li, et al. Online Extrinsic Parameter Calibration for Robotic Camera–Encoder System. *IEEE Transactions on Industrial Informatics*, 2019, 15(8): 4646-4655. doi:10.1109/tii.2019.2894106.
11. J-S Rigoberto, G L N. and D-R V H. Single-shot camera position estimation by crossed grating imaging. *Optics Communications*, 2017, 382: 585-594. doi:10.1016/j.optcom.2016.08.041.
12. Z Zhang. A flexible new technique for camera calibration. *IEEE Transactions on Pattern Analysis and Machine Intelligence*, 2000, 22(11): 1330-1334. doi:10.1109/34.888718.
13. R Y Tsai and R K Lenz. A new technique for fully autonomous and efficient 3D robotics hand/eye calibration. *IEEE Transactions on Robotics and Automation*, 1989, 5(3): 345-358. doi:10.1109/70.34770.
14. S-H Chiu, J-J Liaw and K-H Lin. A Fast Randomized Hough Transform for Circle/Circular Arc Recognition. *International Journal of Pattern Recognition and Artificial Intelligence*, 2011, 24(03): 457-474. doi:10.1142/s0218001410007956.
15. A O Djekoune, K Messaoudi and K Amara. Incremental circle hough transform: An improved method for circle detection. *Optik*, 2017, 133: 17-31. doi:10.1016/j.ijleo.2016.12.064.

Figures

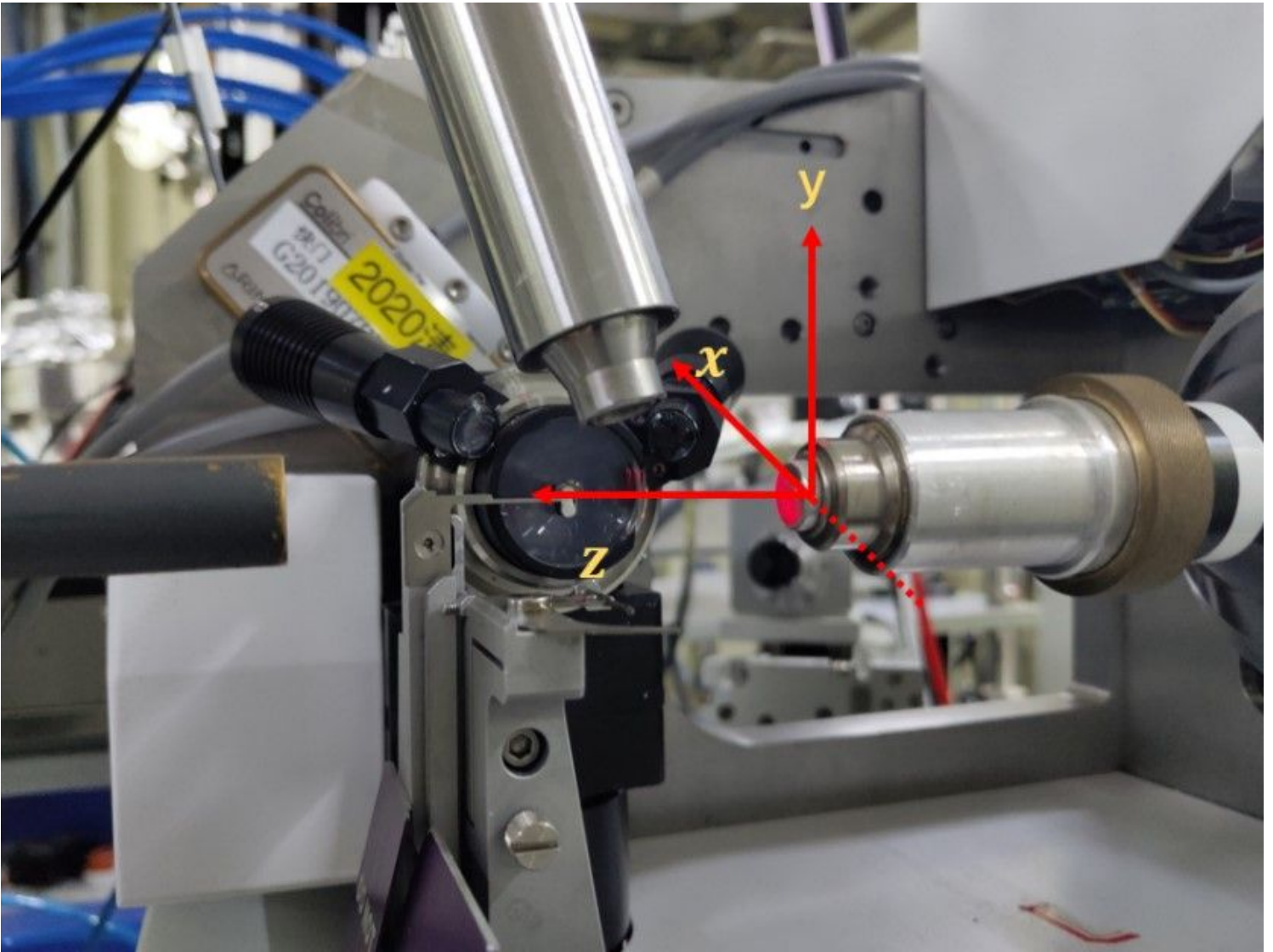


Figure 1

Relative motion coordinate system of robot and goniometer

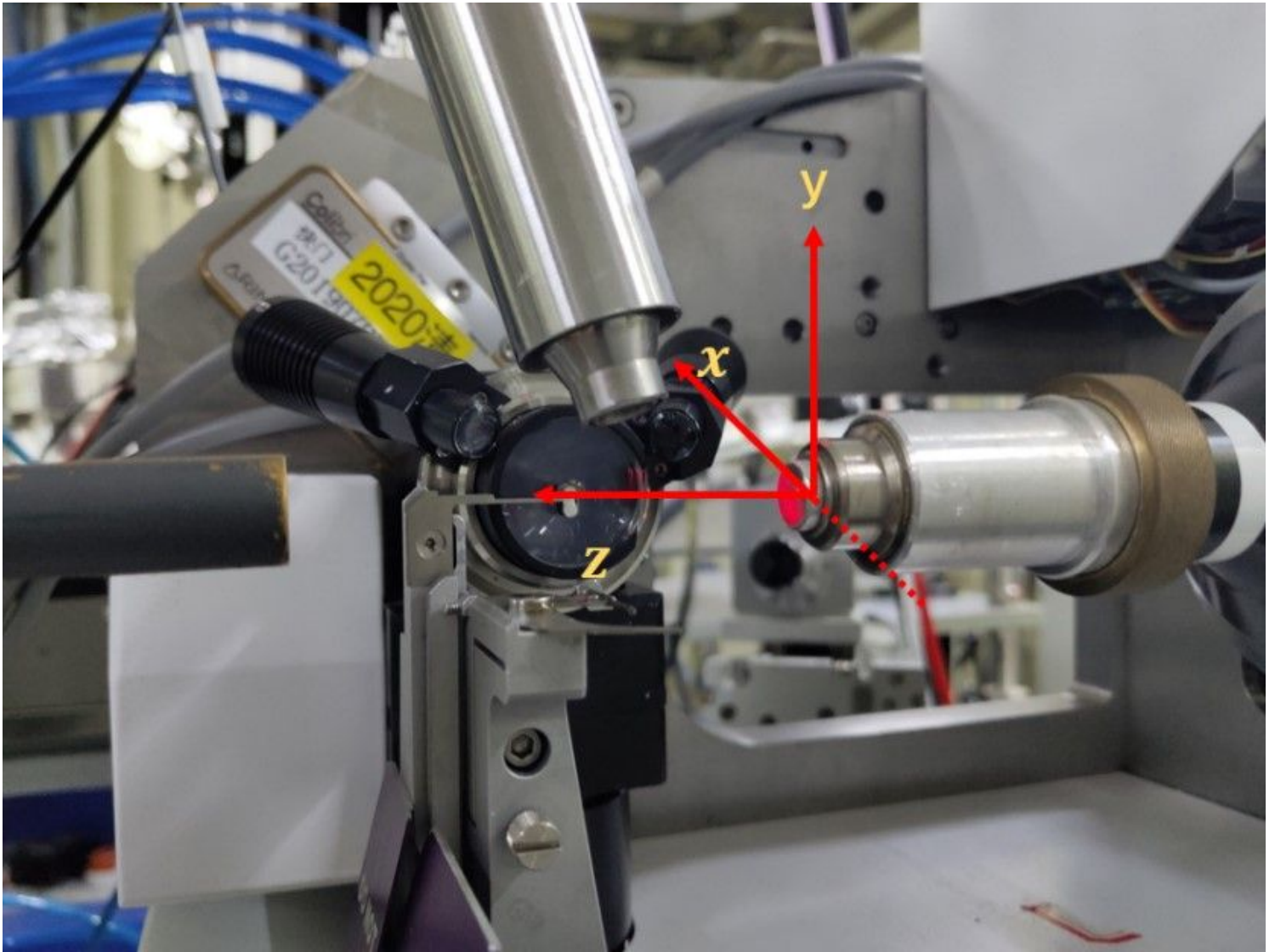


Figure 1

Relative motion coordinate system of robot and goniometer

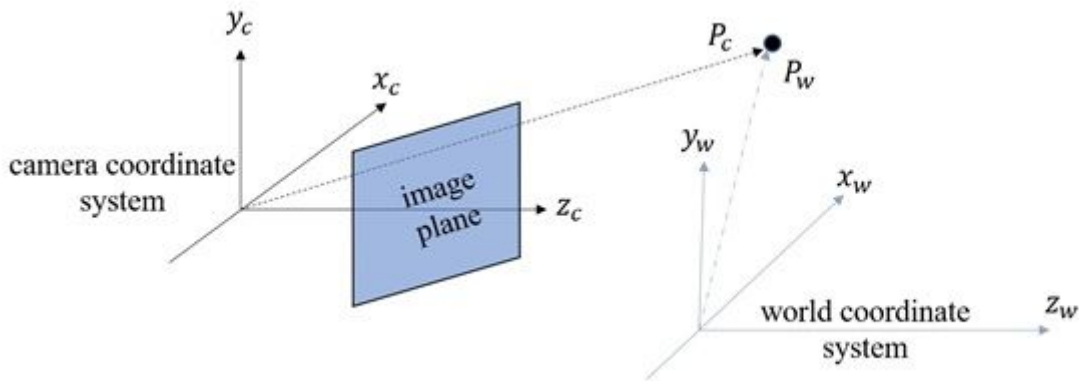


Figure 2

Schematic diagram of camera imaging model

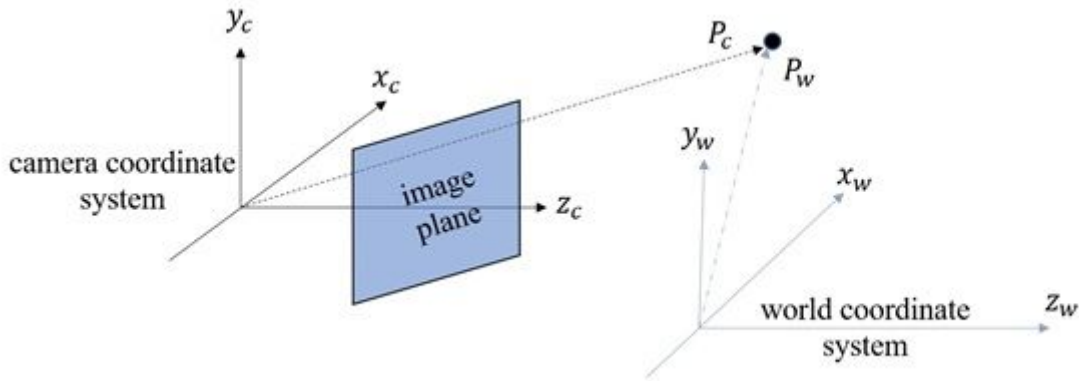


Figure 2

Schematic diagram of camera imaging model

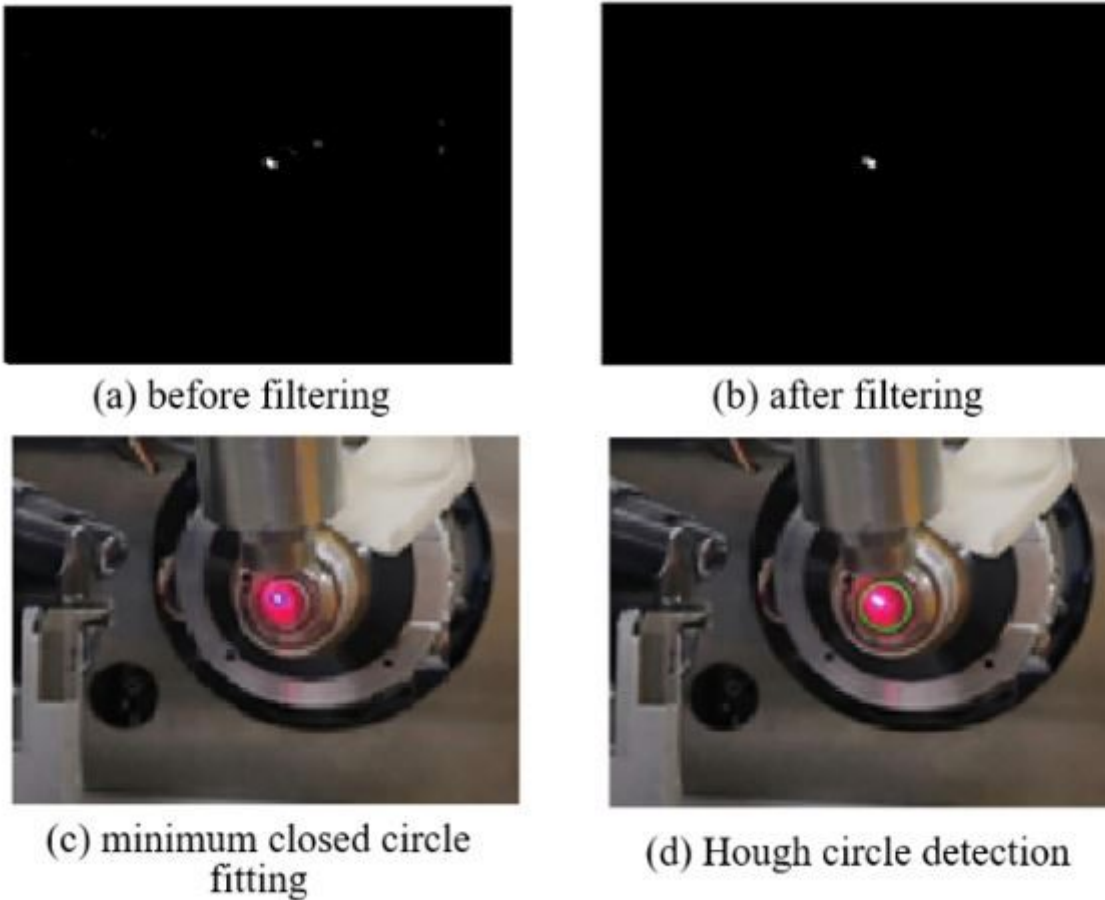
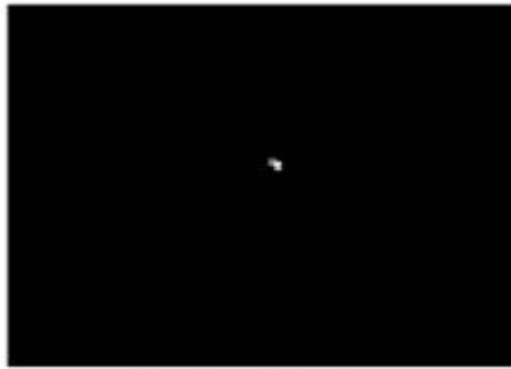


Figure 3

Positioning images of laser spot and goniometer. (a) and (b) are respectively the positioning image of the laser spot before and after filtering. (c) and (d) are respectively the positioning image of goniometer with different detection algorithms



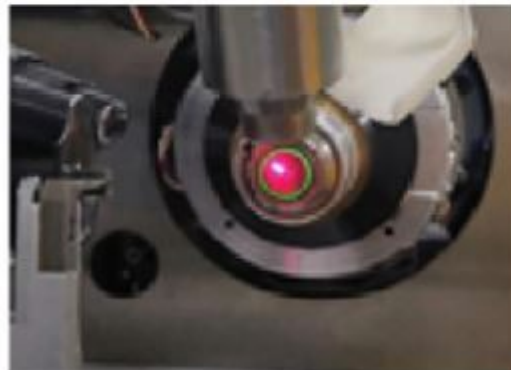
(a) before filtering



(b) after filtering



(c) minimum closed circle fitting



(d) Hough circle detection

Figure 3

Positioning images of laser spot and goniometer. (a) and (b) are respectively the positioning image of the laser spot before and after filtering. (c) and (d) are respectively the positioning image of goniometer with different detection algorithms

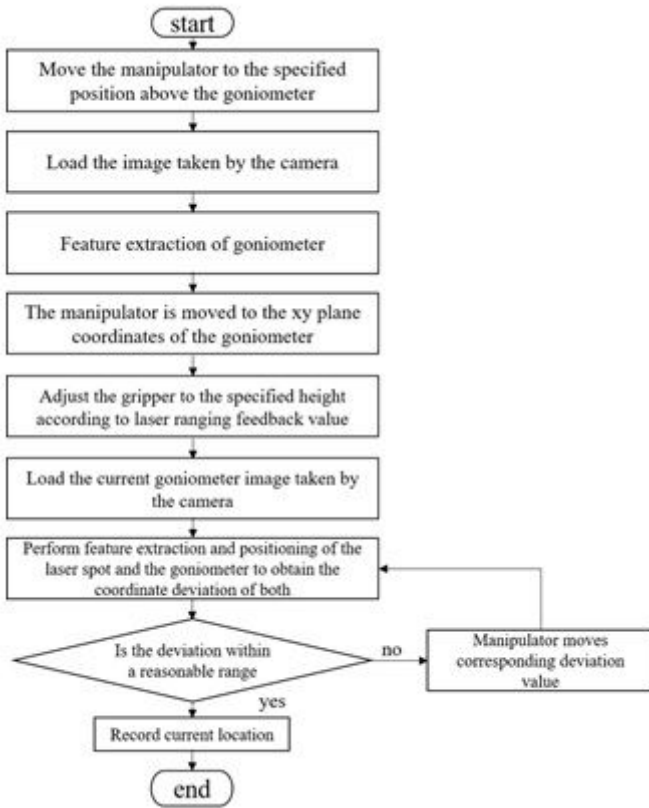


Figure 4

Block diagram of control flow for automatic calibration of goniometer position

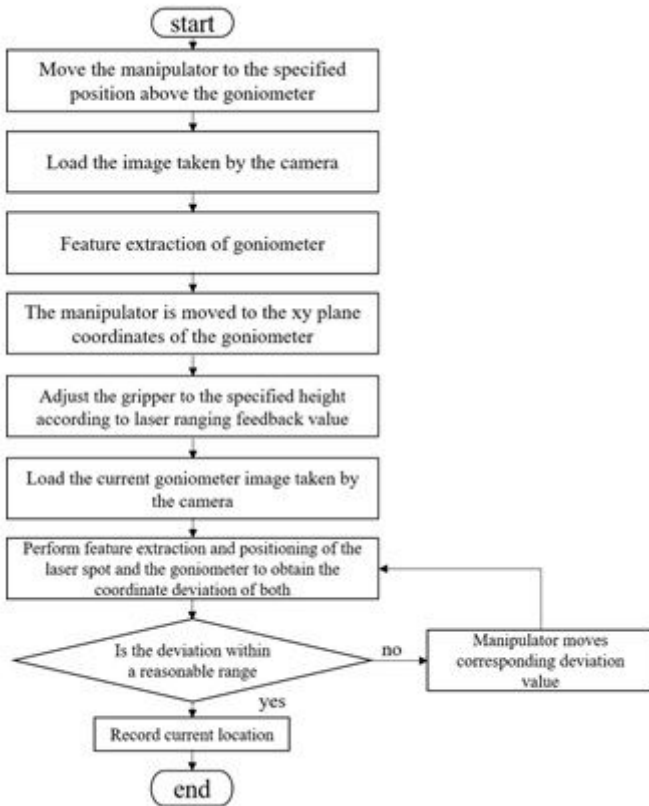


Figure 4

Block diagram of control flow for automatic calibration of goniometer position